INTERNATIONAL JOURNAL FOR NUMERICAL METHODS IN BIOMEDICAL ENGINEERING
Int. J. Numer. Meth. Biomed. Engng. 2015; e02712
Published online 10 April 2015 in Wiley Online Library (wileyonlinelibrary.com). DOI: 10.1002/cnm.2712

Finite element evaluation of the effect of fingertip geometry on contact pressure during flat contact

Gregor Harih[1,*,†] and Mitsunori Tada[2]

[1]*Laboratory for Intelligent CAD Systems, Faculty of Mechanical Engineering, University of Maribor, Smetanova ulica 17, Maribor SI-2000, Slovenia*
[2]*Digital Human Research Center, National Institute of Advanced Industrial Science and Technology, Japan*

SUMMARY

Several studies investigated the mechanical loads developing in the hands during the use of various products in order to enhance user's performance, increase satisfaction and lower the risk of acute and cumulative trauma disorders. Values of pressure discomfort (PDT) and pressure-pain threshold (PPT) were, hence, provided. PDT and PPT may differ significantly for each subject and area of the hand because of psychological and physiological factors. A finite element study of the effect of fingertip anthropometry and anatomy geometry on mechanical loads developed during grasping is carried out in this research in order to assess physiological aspects behind variations of PDT and PPT existing between different subjects. It is found that the underlying anatomical structure and geometry (especially of the bone) significantly affect contact pressure distributions and pressure peak values. The largest difference in peak contact pressure between two different fingertips was in fact 27% for the same applied force. Furthermore, contact pressure distributions varied significantly between different subjects. The findings of this research provide novel insight into the phenomena of human grasping and the variation of contact pressure from subject to subject. Copyright © 2015 John Wiley & Sons, Ltd.

Received 14 August 2014; Revised 18 February 2015; Accepted 18 February 2015

KEY WORDS: fingertip geometry; contact pressure; contact simulation; finite element method; pressure discomfort threshold; pressure pain threshold

1. INTRODUCTION

Significant attention has been given to products in terms of perceived comfort/discomfort. It has been shown that comfort is strongly correlated to user performance, satisfaction and injury frequency [1–3]. Comfort is affected by physical, physiological and psychological factors, and is subjectively defined by feelings that differ from subject to subject [4]. In order to reduce discomfort, the designers must optimise the human-product interaction [5]. Comfort may be increased by optimising the functionality of the product and the physical interaction between the hand and the product. There is also a correlation between the actual properties and psychophysically sensed properties of the materials touched by the users [6].

Unlike conventional engineering materials, human skin and subcutaneous tissue are highly complex structures, therefore their material properties are, in many cases due to ethical issues, hard to measure and define. The mechanical properties of skin and subcutaneous tissue have been extensively investigated by many researchers using different approaches and sample preparation techniques [7–13]. It has been shown that skin and subcutaneous tissue have non-linear viscoelastic

*Correspondence to: Gregor Harih, LICADS - Laboratory for Intelligent CAD Systems, Faculty for Mechanical Engineering, University of Maribor, Maribor SI-2000, Slovenia.
†E-mail: gregor.harih@um.si

properties, where the skin is stiffer than the subcutaneous tissue. Both have low stiffness regions during small strains followed by substantial increase in stiffness as the strain increases.

According to this mechanical behaviour and to human sensation, it is necessary to avoid high contact pressures. By increasing the grasp contact area, it is possible to reduce contact pressure at a given grasp force. This leads to basic ergonomic design recommendations [14–19]. However, some authors have argued that increasing contact areas can reduce the subjective comfort rating because more pressure sensors are triggered within the soft tissue [20, 21].

Rough guidelines of pressure discomfort (PDT) and pressure-pain threshold (PPT) have been provided, where PPT is higher than PDT. The values of these parameters also differ according to the area of the hand and between different subjects [22]. The PDT limit of 188 kPa has been reported by Aldien *et al.* [22], however Fransson-Hall and Kilbom [23] estimated the value as 104 kPa. It has been shown that localised peak pressures vary with handle size and shape as well as they depend on applied grip/push forces. Authors have suggested that a product's handle should identify the handle's size and shape in order to distribute the contact pressure more evenly thus maintaining the desired user's satisfaction and performance.

It has already been shown that cellular materials can be characterised to meet specific mechanical behaviour [24, 25]. Within such context, we have already proposed a composite cellular foam material that can lower the contact pressure while keeping the low deformation rate of the tool-handle material to maintain a sufficient stability rate when handling, as the proposed foam material takes into account the non-linear behaviour of fingertips' soft tissues [16].

Finite element simulations have proved that the contact pressure in the fingertip is significantly affected by surface curvature [26]. The objects following the shape of the fingertip and the skin's surface result in much lower contact pressures and local deformation of the skin and subcutaneous tissue, which can prevent discomfort. However, it has not been shown as to what extent anatomical structures and their geometries contribute to the resulting load.

Many researchers have argued that it is preferable to use subjective measurement methods such as testing of the product using targeted populations and questionnaires, when evaluating a hand-held product, as comfort ratings are subjectively defined [1]. However, this method gives only the resulting comfort rating but does not provide any insight into the physiological aspect of the mechanical load on comfort and the difference between subjects. Subjective methods also have clear disadvantages such as time error and context effects [27].

The aim of this research was to investigate the physiological factors regarding the difference of PDT and PPT limits between subjects. We used commercial finite element software to model and simulate a human fingertip's contact with a flat object. We investigated the influence of fingertip anthropometry and anatomy on contact pressure and its distribution during flat contact using three different three-dimensional (3D) fingertip models based on reconstructed medical images of three test subjects. We observed whether there are any differences between different fingertip geometries in peak contact pressure values as well as contact pressure distributions, which could explain the differences in PDT and PPT between subjects.

2. FINITE ELEMENT MODELLING AND ANALYSIS

2.1. Finite element model – geometrical and boundary conditions

The 3D finite element models of three different human fingertips (Figure 1) were reconstructed from medical images [28]. The magneti resonance (MR) volume data of the index fingertips of three healthy male subjects aged from 25 to 32 were therefore acquired. The images were obtained using a 4.7 T, 230 mm bore MRI scanner (Unity INOVA, Varian, Inc., Palo Alto, California, USA). The volume data was obtained using a 3D gradient echo sequence with repetition time (TR)/echo time (TE) of 20/10 m/s, the field of view was $120x30x30$ mm^3 and volume size was $512x128x128$ voxels. Resolution of the volume data was thus 234 μm/voxels. It took about 5 min to obtain a volume data for one subject. The preprocessed volumes were manually segmented into four sections to generate finite element models including interfaces between different materials. The contact between bone and soft tissue has been simplified using sections where material properties change accordingly.

DOI: 10.1002/cnm

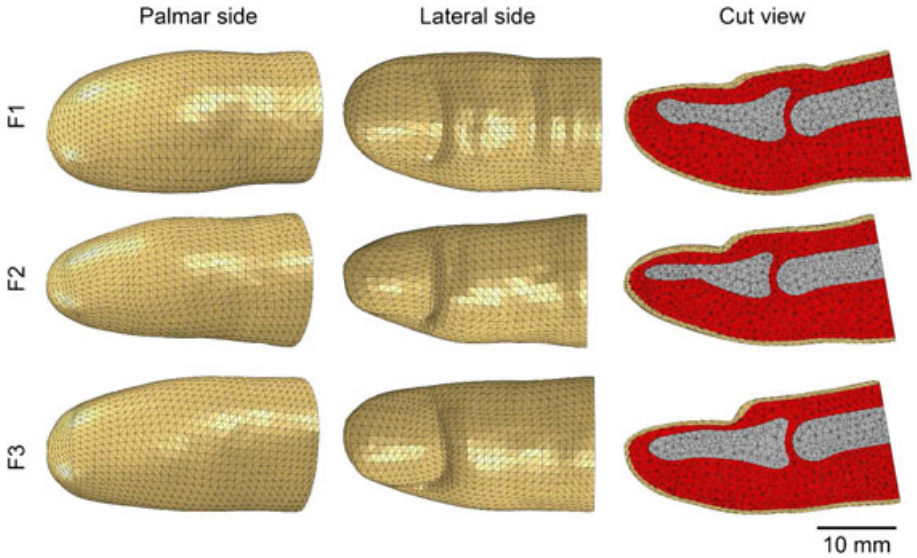

Figure 1. Comparison of anatomy and geometry of the three fingertips analysed in this study.

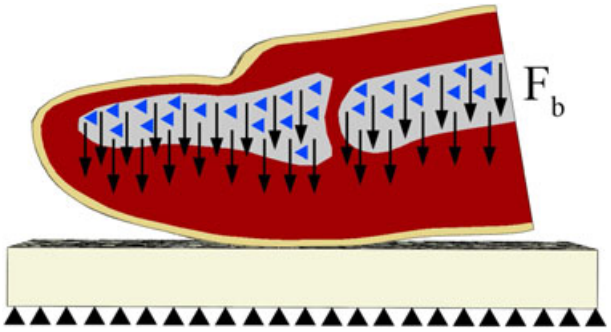

Figure 2. Geometrical and boundary conditions.

The fingertip models F1, F2 and F3 were meshed using 56088, 44730 and 48559 C3D4 elements, respectively. The size of the mesh had been determined to provide a reasonable compromise between computing time and the accuracies of the results based on a performed convergence analysis.

No statistical analysis was performed on the fingertips geometries; however, according to qualitative descriptions relative to each fingertip, fingertip F1 could be considered as fat, F2 as slim and F3 as a normal fingertip (closest to the 50th percentile).

A flat block representing a simplified object's surface was modelled and meshed using 40164 C3D4 elements. It was placed in contact with the fingertip. Hard contact was considered with a friction coefficient of 1. Displacements and rotations of the block were fixed on the lower surface (Figure 2). The displacement and rotations of the fingertips were fixed, except for the displacement along the vertical axis. The load was evenly distributed as a body force (F_b) applied on the bones of the fingertip with the vector showing towards the object's surface. As we were considering a quasi-static problem, we conducted implicit analysis.

2.2. Finite element model – material parameters

Fingertip bone was assumed to be linear elastic with isotropic material parameters with Young's modulus of 17 GPa and with a Poisson ratio of 0.3 [29]. As skin and subcutaneous tissue show more complex non-linear behaviour, we used the Ogden hyper-elastic material model based on data from a uniaxial tensile test (Appendix, Table A.I and A.II) [9]. Skin and subcutaneous tissue are almost incompressible. However, in order to maintain the desired convergence of the numerical tests, the

DOI: 10.1002/cnm

Poisson ratio was set at 0.4 [29]. We considered quasi-static simulations with low deformation rates, therefore the viscosity of the soft tissue was unconsidered in our simulations.

In order to be able to evaluate the differences between the mechanical responses of different fingertips, we used a rigid material model for the object that was in contact with the fingertip.

2.3. *Finite element model – numerical tests*

The commercial finite element code Abaqus/CAE 6.10 (Dassault Systems, France) was utilised in this study.

In order to investigate the physiological aspects of the different levels of comfort between subjects, finite element (FE) simulations were carried out with values of finger force such as to generate values of highest contact pressure equal to 40, 80, 120 and 160 kPa, respectively. These values were relative to fingertip F3, which was closest to the 50th percentile human fingertip anthropometry. The same force values were then given as inputs into the FE models of fingertips F1 and F2. The largest value of contact pressure (i.e. 160 kPa) was chosen based on the limit values of PDT and PPT reported in literature. The other load cases were added in order to gather further information on the fingertip/flat objects contact behaviour.

Contact pressure distribution was computed for each fingertip's geometry and applied force value. As pressure distribution is relative to a given load-case, we showed also the variation in the peak contact pressure with respect to the normalised fingertip force and the vertical fingertip displacement. These data were obtained by continuously increasing fingertip force up to its maximum value. This allowed continuous monitoring of the fingertips' mechanical responses during contact and compare the relative behaviour of fingertip geometries at any load levels (i.e. from zero to the normalised force of 1). Finger force values were normalised with respect to the highest value of finger force used during the FE simulations.

2.4. *Verification of the FE model*

Validation of FE models developed for biological systems is very difficult as material models are determined *in vitro* and thus do not represent the actual mechanical behaviour of living material within the biological systems. At the same time, the material properties for the same biological structures can differ from person to person. The geometries of the observed structures also have a major impact as individual anthropometric measurements vary from person to person. Therefore, validation as it is known from classical mechanical engineering practice is impossible within simulations of biological systems. Despite this fact, we verified and validated our previously developed

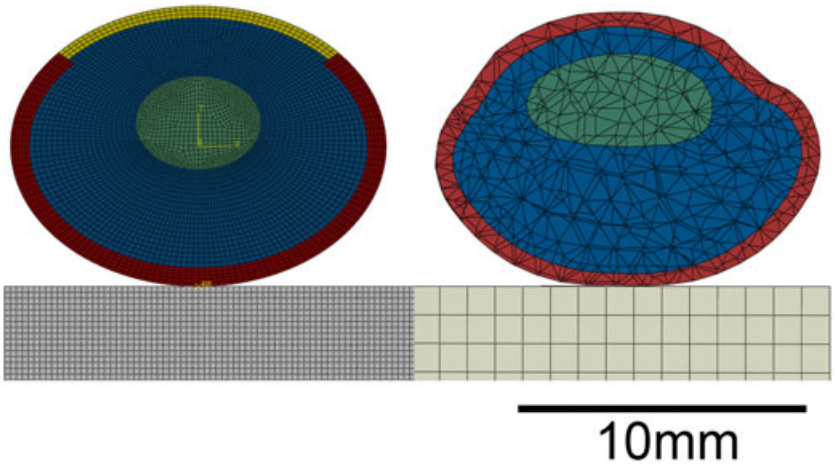

Figure 3. Comparison of the 2D fingertip FE model and corresponding cross section of the 3D fingertip FE model.

DOI: 10.1002/cnm

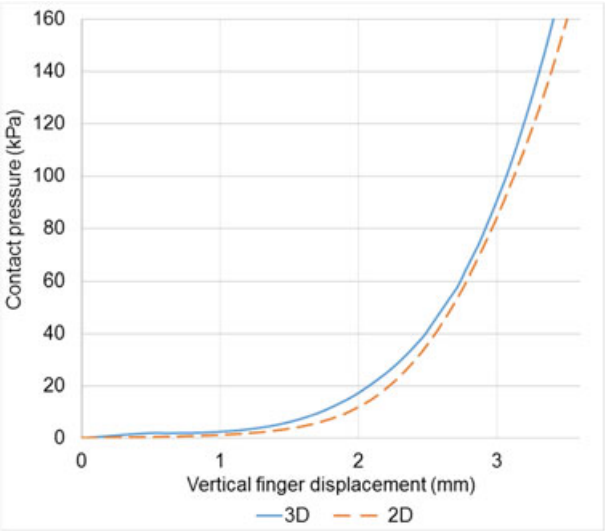

Figure 4. Continuous variation of peak contact pressure with respect to the vertical fingertip displacement.

two-dimensional (2D) FE model against experimental data and other FE models [16, 26, 29, 30]. In order to compare the 3D FE model in terms of peak contact pressure, we analysed the continuous variation of peak contact pressure with respect to the vertical displacement of the 50th percentile fingertip at increasing loads in comparison with our validated simplified 50th percentile 2D FE model. The displacement for obtaining 160 kPa of peak contact pressure using the 3D FE model was determined at the corresponding cross section most similar to the 2D FE model (Figure 3).

The results of validation showed very good agreement in terms of continuous variation of peak contact pressure with respect to the vertical fingertip displacement (Figure 4). Slight differences in values and shapes were found because of the geometrical simplification of the 2D model [31]. As commercial pressure mapping systems do not allow reliable measurements of such small differences in contact pressure and contact area, we were unable to validate our 3D fingertip models in terms of contact pressure distribution [32, 33].

3. RESULTS

Distributions of contact pressures at the objects' surfaces computed by ABAQUS for each fingertip geometry and loading case are shown in Figure 5 through 8. Figure 5 presents the FE results obtained for the vertical force value generating a peak contact pressure of 40 kPa in fingertip F3 (the same vertical force value was also utilised for fingertips F1 and F2). The highest contact pressures were raised to 52 and 41 kPa, respectively, for fingertips F1 and F2.

In order to easily compare contact pressure distributions and values of peak pressure computed by ABAQUS for different load cases, the contact pressure scale (i.e. CPRESS) was set with respect to the maximum peak contact pressure computed for the largest vertical force given in input to the FE model.

Figure 6 shows the FE results obtained by setting the vertical force equal to that generating an 80 kPa peak contact pressure in fingertip F3. The resulting maximum contact pressure evaluated for fingertips F1 and F2 is 104 and 84 kPa, respectively. It can be seen from the figure that differences in contact area and pressure distribution emerge.

Figure 7 shows the FE results obtained by setting the vertical force equal to that generating 120 kPa peak pressure in fingertip F3. The resulting maximum contact pressure evaluated for fingertips F1 and F2 is 154 and 125 kPa, respectively.

Finally, peak contact pressure values raised to 203 and 166 kPa, respectively, for fingertips F1 and F2, when the vertical force was set to its maximum nominal value (i.e. that generating 160 kPa peak contact pressure in fingertip F3; Figure 8).

DOI: 10.1002/cnm

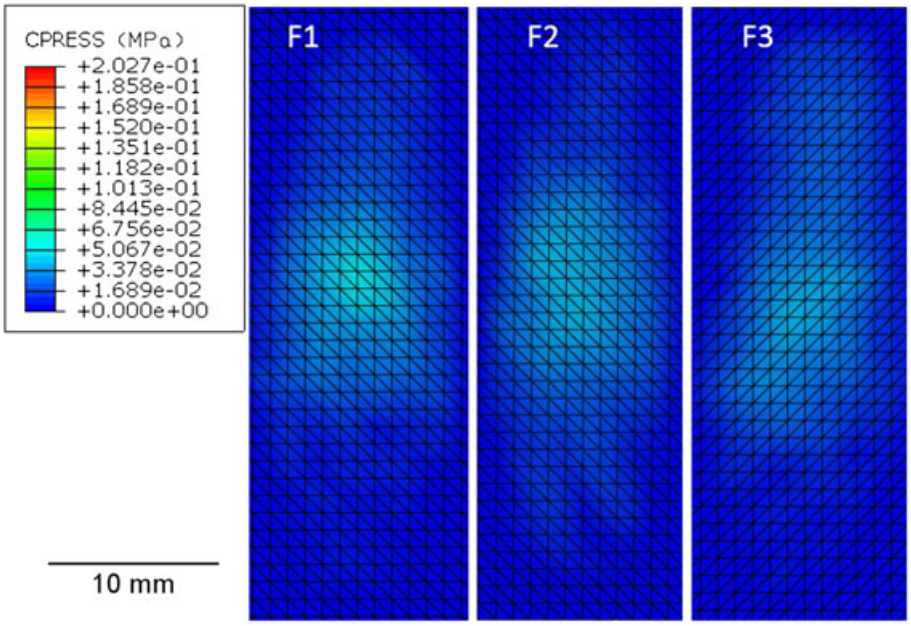

Figure 5. Distributions of contact pressure evaluated for the vertical force generating a 40~kPa peak contact pressure in fingertip F3.

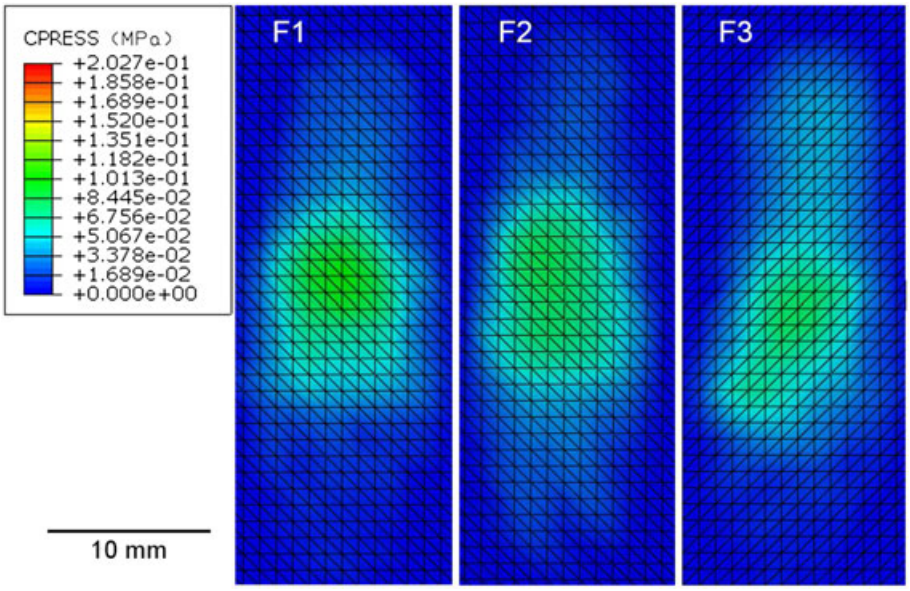

Figure 6. Distributions of contact pressure evaluated for the vertical force generating an 80 kPa peak contact pressure in fingertip F3.

The variation of contact pressure with respect to normalised finger force also was analysed (Figure 9). There is almost linear correlation between the maximum contact pressure and the normalised finger force. While fingertips F2 and F3 had almost the same response, fingertip F1 showed significantly higher contact pressures at given values of normalised finger force.

Figure 10 shows the variations in contact pressures with respect to the fingers' vertical displacements. Fingertips F2 and F3 showed almost the same behaviour, where the latter had a slightly larger finger vertical displacement at the given contact pressure. The mechanical response of fingertip F1

DOI: 10.1002/cnm

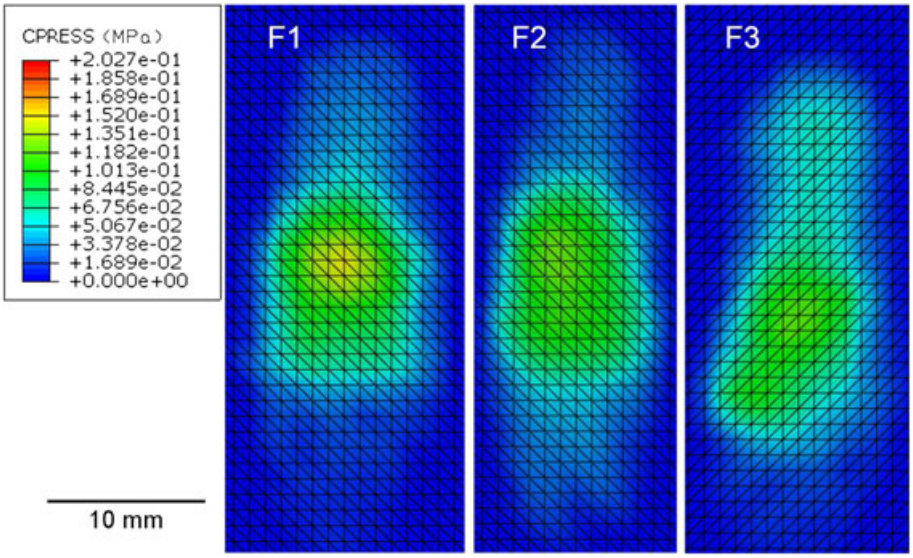

Figure 7. Distributions of contact pressure evaluated for the vertical force generating a 120 kPa peak contact pressure in fingertip F3.

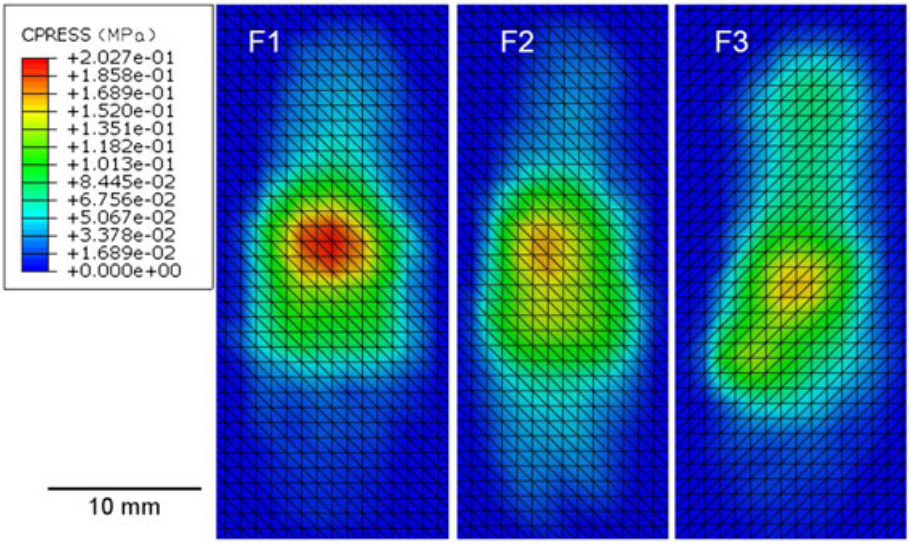

Figure 8. Distributions of contact pressure evaluated for the vertical force generating a 160 kPa peak contact pressure.

was almost the same as F2 and F3 until about 3 mm vertical displacement of the finger. Afterwards, fingertip F1 produced significantly larger displacement than the other two geometries.

4. DISCUSSION

This study analysed the distribution of contact pressure between fingertips and flat object for different fingertip geometries and load levels. The results from finite element analyses showed uneven distributions of contact pressure thus confirming that 2D fingertip models cannot be used to simulate the mechanical behaviour of a 3D human fingertip because contact pressure distribution also varies in the longitudinal direction.

Contact pressures were found to be different already when corresponding to the lowest vertical force imposed on the models (i.e. that which generates a 40 kPa peak contact pressure in

DOI: 10.1002/cnm

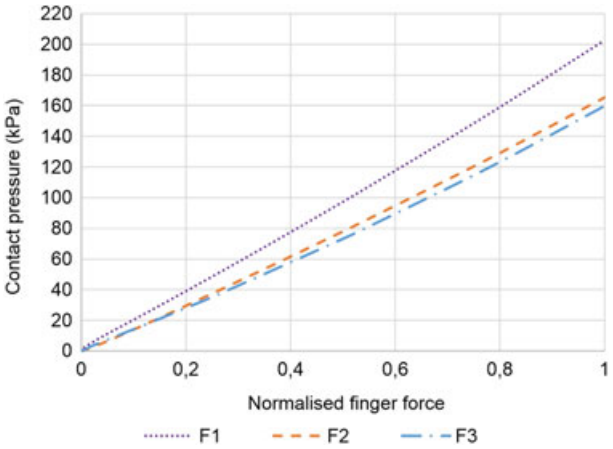

Figure 9. Variation of peak contact pressure with respect to normalised finger force.

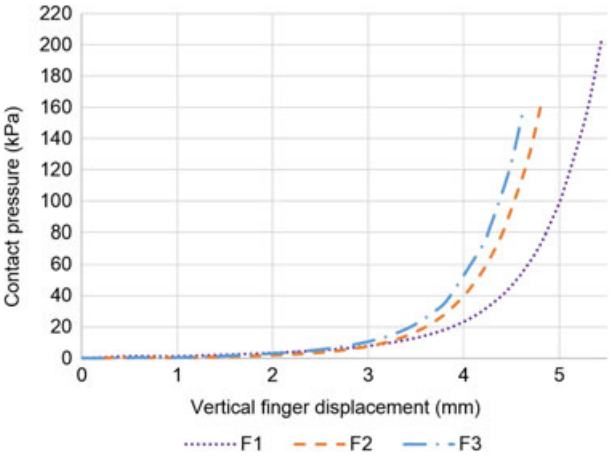

Figure 10. Variation of peak contact pressure with respect to vertical finger displacement.

fingertip F3). The highest contact pressure was obtained for fingertip F1 that included a smaller contact area than fingertips F2 and F3. The smallest pressure was determined for fingertip F3 where the contact area became larger especially towards the finger's end. Furthermore, the cut view of Figure 1 shows that the shape of the F1 finger pad (this small area is the first to come in contact with the object's surface) is convex. As this area is smaller than those of the other finger pads, which are almost flat (F2 and F3), a higher contact pressure developed in fingertip F1.

The differences in contact pressure distribution became more evident for the next load case where vertical force produced a peak contact pressure of 80 kPa in fingertip F3 (Figure 6). Fingertip F1 produced the highest contact pressure due to the smaller contact area and non-uniform stress distribution. The contact areas and pressure distributions of fingertip F3 were completely different from those computed for fingertips F1 and F2. However, the peak contact pressures computed for F2 and F3 were only slightly different. This was due to the very uniform contact pressure distribution exhibited by fingertip F2. Again, the mechanical response was strictly dependent on fingertip geometry.

The maximum contact pressure computed when the applied vertical force generated a peak pressure of 120 kPa in fingertip F3 was 154 kPa for fingertip F1. Such a large difference can be explained when looking at Figure 7: contact area of fingertip F1 is smaller and pressure distribution is less homogeneous than in the case of fingertip F3, similarly to what was observed for the previous loading cases. The peak contact pressures computed for F2 and F3 were again slightly different (i.e. 125 kPa vs. 120 kPa), although the corresponding pressure distributions varied by a greater extent.

DOI: 10.1002/cnm

Fingertip F2 again showed an oval-like contact area with more uniform pressure distribution while fingertip F3 showed a longer and narrower contact area and a less homogeneous pressure distribution. Because of the larger deformations of skin and subcutaneous tissue, the stresses also increased and the contact pressure distributions became different.

The final load case was set to produce 160 kPa in the normal fingertip F3. The highest contact pressure was again obtained for fingertip F1: 203 kPa, which was 43 kPa higher than its counterpart for fingertip F3. The difference in peak contact pressure between fingertips F1 and F3 was almost 27%. As the peak contact pressure of 160 kPa was chosen based on the limit values of PDT and PPT quoted in literature, the results obtained in this study (e.g. the 203 kPa peak contact pressure computed for fingertip F1) may provide information on the level of pain/discomfort caused by objects' handling. The peak pressure computed for fingertip F2 was slightly higher than that computed for fingertip F3 (i.e. 166 kPa vs. 160 kPa). This load case confirmed the trend observed for the other load levels; the distribution of contact pressure was less homogeneous for fingertip F1. Inspite of the similarity in shape of the contact areas between fingertips F1 and F2, contact pressure distribution and peak contact pressure were significantly different; in particular, contact pressure was more

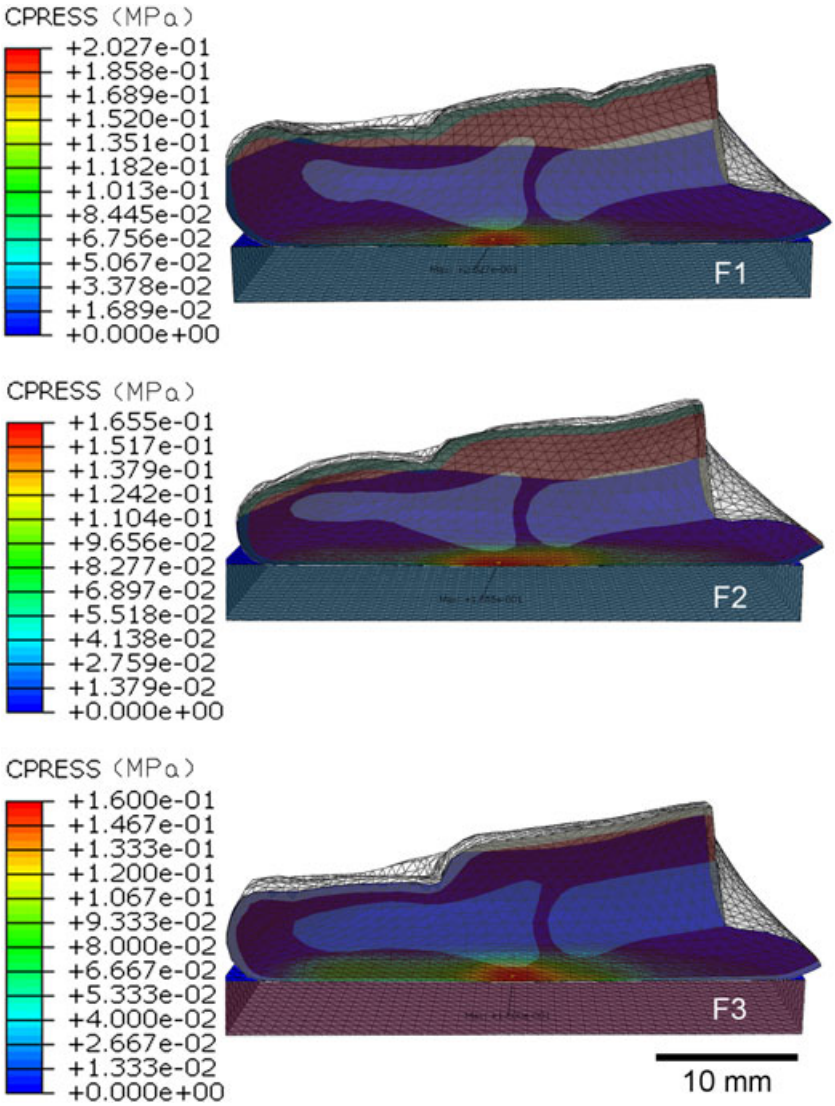

Figure 11. Cut views of pressure distribution computed for each fingertip anatomy in correspondence of the largest applied load.

DOI: 10.1002/cnm

evenly distributed in fingertip F2. Fingertip F3 again showed significant differences in contact area and pressure distribution (including the location of the pressure peak) from fingertips F1 and F2.

The mechanical responses exhibited by the different fingertips were strictly dependent on fingertip geometries and anatomies. Important information can be gathered from Figure 11 that shows the pressure distribution together with the 3D model in cut view of each fingertip for the maximum vertical force applied to the model. It can be seen that the geometry of skin, subcutaneous tissue and fingertip bones had a significant impact on contact pressure distribution and peak contact pressure. At the lowest load, the shape of soft tissue had higher impact on contact pressure distribution as this part of the finger started to deform first as it was the softest material within the simulated system. However, at the higher loads, which are more critical for the development of various cumulative traumatic disorders, bone size and shape becomes more important as the soft tissue is already deformed. In the presented case, the distal phalange bone of fingertip F1 was smaller and shorter than in the cases of fingertips F2 and F3. The cut view also shows that the angle of the lower contour of the bone in fingertip F1 was slightly tilted upwards with respect to fingertip F3. The concave-like distal phalange bone of fingertip F3 with almost no tilt produced uniform contact pressure distribution across the finger length. This happened because the concave distal phalange restricted soft tissue deformation in the longitudinal direction, thus preventing extensive deformation in the longitudinal direction towards the fingertip's end. The shapes of the distal phalange bones of F1 and F2 were similar; however, in the case of fingertip F1, it was smaller and slightly tilted upwards, which explains the higher peak contact pressure and less uniform contact pressure distribution. The higher impact of bone shape and size at peak contact pressure and distribution can also be observed from the higher load-cases (120 and 160 kPa), where contact pressure was more non-uniform compared with the lower load-cases (40 and 80 kPa). The locations of the peak contact pressures at higher load-cases corresponded exactly to that portion of the finger where the bone is closest to the surface. According to literature, we can assume that the difference in contact pressure distributions because of fingertip geometry and anatomy between subjects is the main physiological factor determining the PDT and PPT values [21–23].

In summary, we can observe that for the same finger force the fingertips of different subjects showed completely different mechanical behaviour. For a given finger force, contact pressure distributions and the corresponding peak contact pressures varied considerably for different subjects. In the presented case, the peak pressure of fingertip F1 was significantly higher than for fingertip F3. This can be attributed to the difference in fingertip geometry of soft tissue as well as on the geometry of underlying bones between different subjects.

Figure 9 showed that fingertip F1 produced higher contact pressure than fingertips F2 and F3 for a given normalised finger force. The response curves for fingertips F2 and F3 show similar behaviour. However, both curves have a common intersection at a normalised finger force of about 0.1 because the plots depend on several parameters. The amount of soft tissue and the underlying geometry of the anatomical structure of the bone have a significant impact on the variation of contact pressure with respect to the normalised finger force. At lower contact pressure, the amount of soft tissue and its geometry have a greater influence on the contact pressure. Conversely, at higher contact pressure, when the soft tissue is already deformed, fingertip bone anatomy and its geometry drive the distribution of contact pressure. Therefore, it is necessary to carry out numerical simulations where geometry is correctly defined and realistic material models are given as input into the model.

The peak contact pressure versus finger displacement curves in Figure 10 showed the characteristic behaviour of the hyper-elastic skin and subcutaneous tissue. At lower displacements, the increase of contact pressure with respect to fingertip vertical displacement was relatively small. However, after a certain strain rate, the stiffness of the soft tissue became higher for larger vertical displacements and the contact pressure also started to increase sharply. The plots relative to fingertips F2 and F3 were very similar and significantly different from the trend seen for F1. As fingertip F1 can be considered as a thick finger, it had significantly more soft tissue than fingertips F2 and F3 and its deformation and vertical displacement were larger than for fingertips F2 and F3.

DOI: 10.1002/cnm

5. CONCLUSION

This paper presented a finite element study on the influence of fingertip anthropometry and bone geometry on the mechanical responses of fingertips during flat contacts. The results showed there are major differences in contact pressure distribution and peak contact pressure between different fingertip geometries for a given finger force. The underlying anatomical structure and bone geometry affect the peak contact pressure and contact pressure distribution to a large extent (in the present case, the peak contact pressure varied by 27% between different fingertips). It can therefore be concluded that the variation of contact pressure distribution caused by differences in fingertip geometry/anatomy between subjects is the main physiological factor determining PDT and PPT values. The results presented in this study may hence provide information on the level of pain/discomfort caused by objects' handling. Peak contact pressure values and contact pressure distribution cannot be determined when based only on anthropometry. Realistic numerical simulations should consider a fully 3D fingertip model reconstructed from medical images including correct information on anatomical structure and geometry. The findings of this research may help to better understand human fingertip contact while grasping and the resulting mechanical loads and their effect on the comfort. These information are useful to engineers and ergonomists during the development stages of new handheld products.

Future work should analyse more fingertip geometries to further investigate the effects of fingertip anthropometry and anatomical structure geometry. In addition, subjective responses and pressure mapping should be evaluated and compared with numerical simulations. This would allow full understanding regarding the differences in PDT and PPT values between various subjects. Future work should also consider the variation of material properties of soft tissue, because this would also effect the resulting contact pressure distribution and therefore also PDT and PPT values. Additionally, internal stresses and displacements in other directions could be evaluated providing even deeper insight. The results might be used for developing better handheld products with higher comfort ratings and lower risks of causing cumulative traumatic disorders. This study investigated the contact between a fingertip and a flat block; however, products usually have curved surfaces to allow better fit to the hand. Therefore, future research should also investigate contact with curved surfaces as the contact pressure distributions would be different. Additionally, FE models of subjects, which already show the symptoms of cumulative traumatic disorders, could be modelled and analysed. Future work should also consider the development of a whole hand FE model for analysing the peak contact pressure and its distributions over the whole hand.

APPENDIX

The behaviour of skin and subcutaneous tissue can be described using hyper-elastic material models, where one of the more used is the Ogden strain energy potential [34]:

$$U = \sum_{i=1}^{N} \frac{2\mu_i}{\alpha_i^2} \left[\bar{\lambda}_1^{\alpha_i} + \bar{\lambda}_2^{\alpha_i} + \bar{\lambda}_3^{\alpha_i} - 3 + \frac{1}{D_i} \left(J^{el} - 1 \right)^{2i} \right] \tag{A.1}$$

where $\overline{\lambda}_i$ are the deviatoric principal stretches; $\overline{\lambda}_i = J^{-\frac{1}{3}} \lambda_i$; λ_i are the principal stretches; N is the number of terms used in the definition of the strain energy function; and μ_i and α_i are temperature-dependent material parameters and describe the shear behaviour of the material, D_i is compressibility, J is the Jacobean determinant and J_{el} is the elastic volume ratio. The initial shear modulus and bulk modulus for the Ogden form are given by:

$$\mu_0 = \sum_{i=1}^{N} \mu_i, \qquad K_0 = \frac{2}{D_1} \tag{A.2}$$

DOI: 10.1002/cnm

Table A.I. Hyperelastic constants of skin tissue.

N	μ_i	α_i
1	−0.07594	4.941
2	0.01138	6.425
3	0.06572	4.712

Table A.II. Hyperelastic constants of subcutaneous tissue.

N	μ_i	α_i
1	−0.04895	5.511
2	0.00989	6.571
3	0.03964	5.262

Compressibility can be defined by the specified non-zero values for D_i, where the Poisson ratio is less than 0.5:

$$D_i = \frac{2}{K_0} = \frac{3(1-2\nu)}{\mu_0(1+\nu)} \tag{A.3}$$

REFERENCES

1. Kuijt-Evers LFM, Vink P, de Looze MP. Comfort predictors for different kinds of hand tools: differences and similarities. *International Journal of Industrial Ergonomics* 2007; **37**(1):73–84.
2. Mundermann A, Stefanyshyn DJ, Nigg BM. Relationship between footwear comfort of shoe inserts and anthropometric and sensory factors. *Medicine and Science in Sports and Exercise* 2001; **33**(11):1939–1945.
3. Kinchington M, Ball K, Naughton G. Relation between lower limb comfort and performance in elite footballers. *Physical Therapy in Sport* 2012; **13**(1):27–34.
4. De Looze M, Kuijt-Evers L, and Van Dieën J. Sitting comfort and discomfort and the relationships with objective measures. *TERG Ergonomics* 2003; **46**(10):985–997.
5. Kuijt-Evers LF, Groenesteijn L, de Looze MP, Vink P. Identifying factors of comfort in using hand tools. *Applied Ergonomics* 2004; **35**(5):453–8.
6. Wongsriruksa S, Howes P, Conreen M, Miodownik M. The use of physical property data to predict the touch perception of materials. *Materials & Design* 2012; **42**(0):238–244.
7. Clark JA, Cheng JC, Leung KS. Mechanical properties of normal skin and hypertrophic scars. *Burns* 1996; **22**(6):443–6.
8. Edwards C, Marks R. Evaluation of biomechanical properties of human skin. *Clinics in Dermatology* 1995; **13**(4):375–380.
9. Pan L, Zan L, Foster FS. Ultrasonic and viscoelastic properties of skin under transverse mechanical stress in vitro. *Ultrasound in Medicine and Biology* 1998; **24**(7):995–1007.
10. Wan Abas WA. Biaxial tension test of human skin in vivo. *Bio-medical materials and engineering* 1994; **4**(7): 473–86.
11. Wilhelmi BJ, Blackwell SJ, Mancoll JS, Phillips LG. Creep vs. stretch: a review of the viscoelastic properties of skin. *Annals of plastic surgery* 1998; **41**(2):215–9.
12. Zheng YP, Mak AF. An ultrasound indentation system for biomechanical properties assessment of soft tissues in-vivo. *IEEE transactions on bio-medical engineering* 1996; **43**(9):912–8.
13. Wu JZ, Cutlip RG, Andrew ME, Dong RG. Simultaneous determination of the nonlinear-elastic properties of skin and subcutaneous tissue in unconfined compression tests. *Skin Research and Technology* 2007; **13**(1):34–42.
14. Kaljun J, Dolšak B. Ergonomic design recommendations based on an actual chainsaw design. *South African journal of industrial engineering* 2012; **23**(2):215–229.
15. Harih G, Dolšak B. Tool-handle design based on a digital human hand model. *International Journal of Industrial Ergonomics* 2013; **43**(4):288–295.
16. Harih G, Dolšak B. Recommendations for tool-handle material choice based on finite element analysis. *Applied Ergonomics* 2014; **45**(3):577–585.
17. Harih G, Dolšak B. Comparison of subjective comfort ratings between anatomically shaped and cylindrical handles. *Applied Ergonomics* 2014; **45**(4):943–954.

DOI: 10.1002/cnm

18. Harih G, Čretnik A. Interdisciplinary approach to tool-handle design based on medical imaging. *BioMed Research International* 2013; **2013**:1–8.
19. Harih G. Decision support system for generating ergonomic tool-handles. *International Journal of Simulation Modelling* 2014; **13**(1):5–15.
20. Goonetilleke RS, Eng TJ. Contact area effects on discomfort. *Proceedings of the Human Factors and Ergonomics Society Annual Meeting Proceedings of the Human Factors and Ergonomics Society Annual Meeting* 1994; **38**(10):688–690.
21. Xiong S, Goonetilleke R, Jiang Z. Pressure thresholds of the human foot: measurement reliability and effects of stimulus characteristics. *Ergonomics* 2011; **54**(3):282–293.
22. Aldien Y, Welcome D, Rakheja S, Dong R, Boileau PE. Contact pressure distribution at hand–handle interface: role of hand forces and handle size. *International Journal of Industrial Ergonomics* 2005; **35**(3):267–286.
23. Fransson-Hall C, Kilbom Å. Sensitivity of the hand to surface pressure. *Applied Ergonomics* 1993; **24**(3):181–189.
24. Vesenjak M, Krstulović-Opara L, Ren Z. Characterization of irregular open-cell cellular structure with silicone pore filler. *Polymer Testing* 2013; **32**(8):1538–1544.
25. Vesenjak M, Borovinšek M, Fiedler T, Higa Y, Ren Z. Structural characterisation of advanced pore morphology (APM) foam elements. *Materials Letters* 2013; **110**(0):201–203.
26. Wu JZ, Dong RG. Analysis of the contact interactions between fingertips and objects with different surface curvatures. *Proceedings of the Institution of Mechanical Engineers, Part H: Journal of Engineering in Medicine Proceedings of the Institution of Mechanical Engineers, Part H: Journal of Engineering in Medicine* 2005; **219**(2): 89–103.
27. Annett J. Subjective rating scales: science or art? *Ergonomics* 2002; **45**(14):966–987.
28. Tada M, Yoshida H, Mochimaru M, Kanade T. Generating subject-specific FE models of fingertip with the use of MR volume registration. In *EuroHaptics 2006*, 2006.
29. Wu JZ, Dong RG, Rakheja S, Schopper AW. Simulation of mechanical responses of fingertip to dynamic loading. *Medical Engineering & Physics* 2002; **24**(4):253–264.
30. Pawluk DT, Howe RD. Dynamic contact of the human fingerpad against a flat surface. *Journal of Biomechanical Engineering* 1999; **121**(6):605–11.
31. Harih G, Kaljun J, Dolsak B. *Comparison of 2D and 3D finite element fingertip during grasping. in: 3rd International Digital Human Modeling Symposium*. Tokyo: Japan, 2014.
32. Lemerle P, Klinger A, Cristalli A, Geuder M. Application of pressure mapping techniques to measure push and gripping forces with precision. *Ergonomics* 2008; **51**(2):168–191.
33. Reinvee M, Jansen K. Utilisation of tactile sensors in ergonomic assessment of hand–handle interface: a review. *Angronomy research* 2014; **12**(3):907–914.
34. Ali A, Hosseini M, Sahari B. A review of constitutive models for rubber-like materials. *American Journal of Engineering and Applied Sciences* 2010; **3**(1):232.

DOI: 10.1002/cnm